Available online at www.sciencedirect.com
SCIENCE DIRECT
Tectonophysics 420 (2006) 283–299
TECTONOPHYSICS
www.elsevier.com/locate/tecto

Lithological interpretation of crustal composition in the Fennoscandian Shield with seismic velocity data

M. Kuusisto [a,*], I.T. Kukkonen [a], P. Heikkinen [b], L.J. Pesonen [c]

[a] Geological Survey of Finland, P.O. Box 96, FIN-02151 Espoo, Finland
[b] Institute of Seismology, PL 68, 00014 University of Helsinki, Finland
[c] Division of Geophysics, PL 64, 00014 University of Helsinki, Finland

Received 14 January 2005; received in revised form 3 October 2005; accepted 4 January 2006
Available online 5 April 2006

Abstract

In this study, we report the results of an investigation of lithological interpretation of the crust in the central Fennoscandian Shield (in Finland) using seismic wide-angle velocity models and laboratory measurements on P- and S-wave velocities of different rock types. The velocities adopted from wide-angle velocity models were compared with laboratory velocities of different rock types corrected for the crustal PT conditions in the study area. The wide-angle velocity models indicate that the P-wave velocity does not only increase step-wise at boundaries of major crustal layers, but there is also gradual increase of velocity within the layers. On the other hand, the laboratory measurements of velocities indicate that no single rock type is able to provide the gradual downward increasing trends. Thus, there must be gradual vertical changes in rock composition. The downward increase of velocities indicates that the composition of the crust becomes gradually more mafic with increasing depth. We have calculated vertical velocity profiles for a range of possible crustal lithological compositions. The Finnish crustal velocity profiles require a more mafic composition than an average global continental model would suggest. For instance, on the SVEKA'81 transect, the calculated models suggest that the crustal velocity profiles can be simulated with rock type mixtures where the upper crust consists of felsic gneisses and granitic–granodioritic rocks with a minor contribution of amphibolite and diabase. In the middle crust, the amphibolite proportion increases. The lower crust consists of tonalitic gneiss, mafic garnet granulite, hornblendite, pyroxenite and minor mafic eclogite. Assuming that these rock types are present in sufficiently extensive and thick layers, they would also have sufficiently high acoustic reflection coefficients for generating the generally well-developed reflectivity in the crust in the central part of the shield. Density profiles calculated from the lithological models suggest that there is practically no density contrast at Moho in areas of the high-velocity lower crust. Comparison of reflectors from FIRE-1 and FIRE-3 transects and the velocity model from SVEKA'81 wide-angle transect indicated that the reflectors correlate with velocity layering, but the three-dimensional structures of the crust complicate such comparisons.

Keywords: Seismic velocity; Crust; Lithology; Petrology; Reflectivity; Density

1. Introduction

Seismic velocities of crystalline rocks are controlled mainly by mineralogical composition, pressure and temperature. To a minor degree, factors such as rock

* Corresponding author.
E-mail address: minna.kuusisto@gtk.fi (M. Kuusisto).

0040-1951/$ - see front matter
doi:10.1016/j.tecto.2006.01.014

texture, anisotropy, porosity and fracturing also influence the velocities. Seismic velocities measured as functions of temperature and pressure are available for a large number of different rock types in the literature (e.g., Kern, 1978; Holbrook et al., 1992; Christensen and Mooney, 1995; Rudnick and Fountain, 1995; Christensen, 1996). In addition, high-quality velocities from seismic wide-angle reflection models are also available from many areas, but lithological interpretation of these crustal velocities is rarely attempted. Christensen and Mooney (1995) and Rudnick and Fountain (1995) compiled global continental crustal velocities derived from wide-angle recordings in different tectonic environments and compared the modelled velocities with rock velocities measured in laboratory. One of the important findings in these studies is that the compositional interpretations derived from velocity information are non-unique, although the problem can be reduced where good quality S-wave velocities are available. Holbrook et al. (1992) documented the bimodal characteristics of P-wave velocities of the lower crust in many tectonic environments suggesting either mafic/ultramafic magmatic activity or high-grade metamorphic processes to be responsible for the observed velocity variations. In a more recent study, Brown et al. (2003), using P- and S-velocities, Poisson ratios, as well as gravity, magnetic and thermal models, were able to show that there are distinct compositional differences in the Urals area between the East European Craton and the Magnitogorsk and East Uralian zones. Using V_P/V_S ratios derived from seismic refraction data in the Grenville and Appalachian provinces in North America, Musacchio et al. (1997) suggested that the high V_P/V_S ratios in the Grenville province are due to gabbroic and anorthositic rocks with high content of plagioclase. Musacchio et al. (2004) estimated the lithosperic composition of the Archaean Superior province with seismic refraction/wide-angle reflection and gravity modelling and indicated that the lower crust is mostly intermediate in composition and would require the presence of 25–60% of granitic rocks.

In this study, we report the results of an investigation aimed at the lithological interpretation of the crust using seismic data in the central part of the Fennoscandian Shield. The study area is challenging because of an anomalously thick crust (52 km on average), a thick high-velocity lower crust and abundance of granitoids in the upper crust (Korja et al., 1993). The crustal evolution of the study area has been summarized by Korsman et al. (1999) and Lahtinen et al. (2005). The evolution of the central part of the Fennoscandian Shield was characterized by break-up of the Archaean craton (ca. 2.2–2.0 Ga ago), opening of an oceanic basin to the west of the craton, and subsequent closure of the oceanic basin and accretion of arcs and micro-continents to the western margin of the craton at about 1.92–1.87 Ga ago. At this stage, major thickening of the lower crust took place. Further south, the southern Finland sedimentary-volcanic complex was accreted to the craton at about 1.885 Ga ago and followed by post-collisional magmatism at 1.80–1.78 Ga ago. The stabilized crust was reactivated at 1.54–1.588 Ga ago when rapakivi intrusions and related magmatism were common in southern Finland (Korsman et al., 1999).

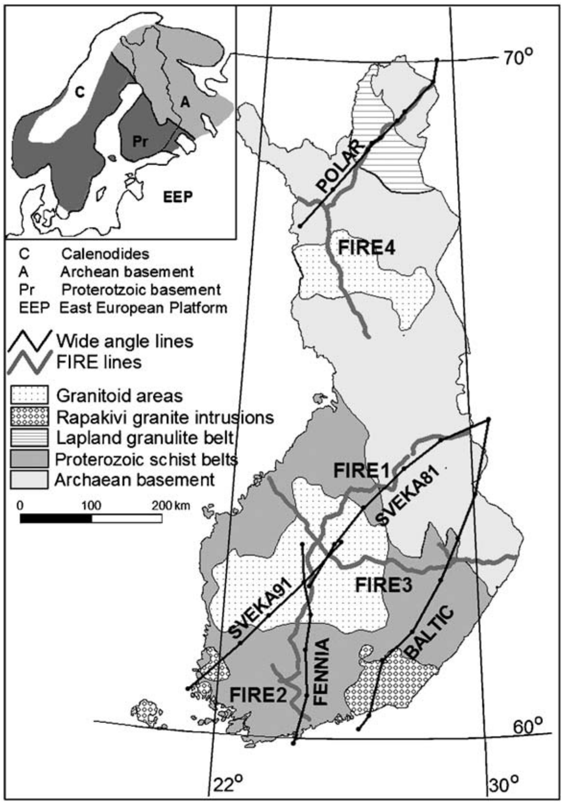

Fig. 1. Locations of seismic wide-angle transects BALTIC, SVEKA'81, SVEKA'91, FENNIA and POLAR (Luosto, 1997), and the FIRE reflection transects (Kukkonen et al., 2004).

Our aim was to investigate the modelled P-wave velocities and V_P/V_S ratios derived from high-quality seismic wide-angle recordings and to compare those velocities with laboratory measurements of velocities of different rock types corrected for the crustal PT conditions appropriate in this part of the shield. Further, we sought trends in the original velocity models suggesting either compositional trends or areal

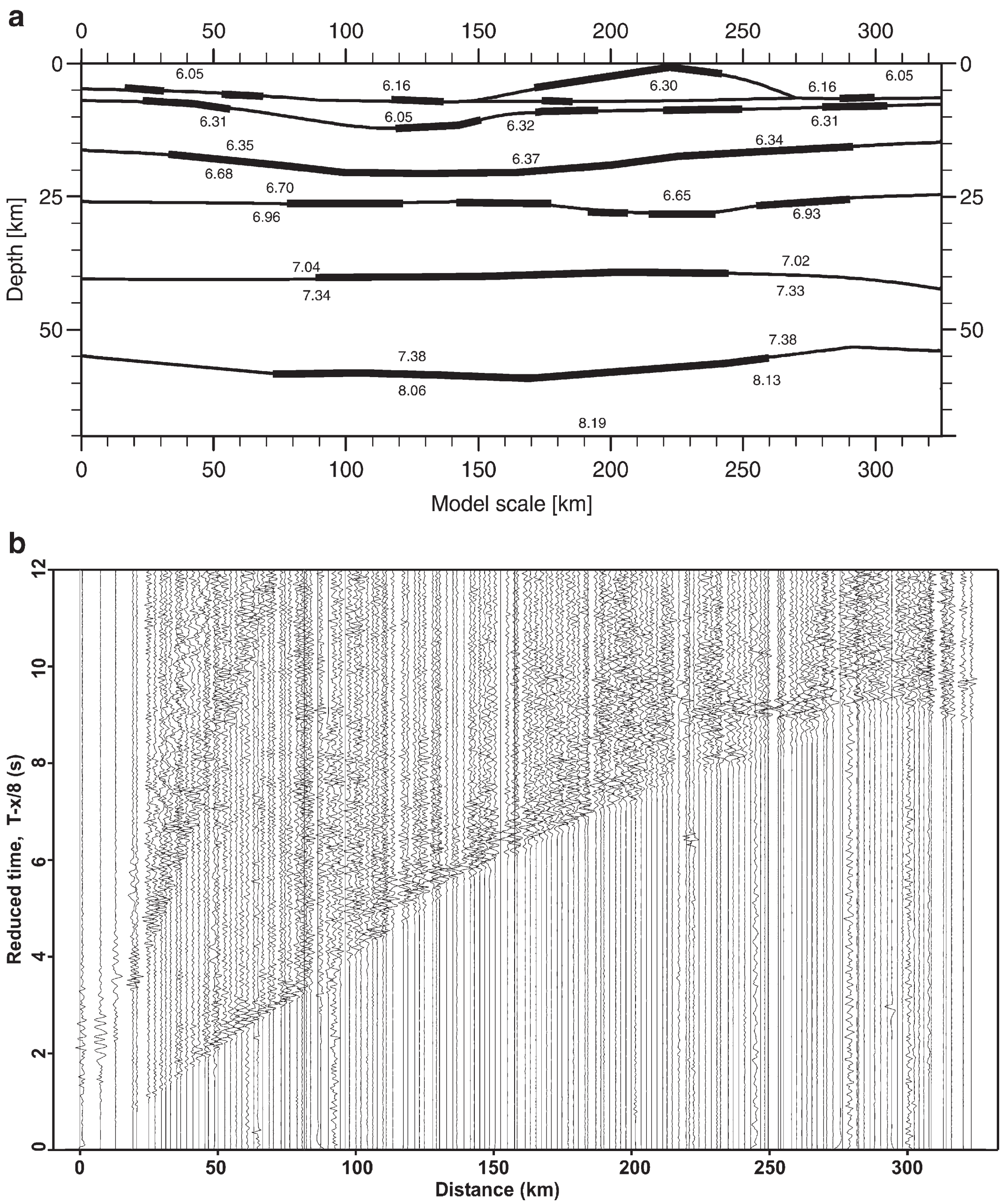

Fig. 2. (a) The ray-tracing velocity model from the deep refraction profile SVEKA'81. The thick lines indicate the parts of the layer boundaries mapped by wide-angle reflections (modified from Grad and Luosto, 1987). (b) The recorded section from the shot point A of SVEKA'81.

differences in the crustal composition. We present quantitative calculations of the crustal composition (rock type mixtures) in the Fennoscandian Shield and ask whether the crustal composition is representative of the global average crustal composition by Christensen and Mooney (1995). We also use lower crustal xenoliths (Peltonen et al., in press; Hölttä et al., 2000) recovered in Finland as indicators of composition. We then use the rock type mixtures to calculate maximum reflection coefficients at different crustal levels. With the help of the lithological models, we calculated density profiles of the crust and discuss the implications on the properties of Moho. Finally, we compare the velocity model of one transect (SVEKA'81) with recent near-incidence reflection sections (FIRE-1 and FIRE-3 transects) in Central Finland.

2. Seismic velocity data: wide-angle model velocities and laboratory measurements

The study area is well covered by previous wide-angle studies, and in the present work we use the results from SVEKA'81, SVEKA'91, FENNIA, BALTIC and POLAR profiles (Fig. 1) (Grad and Luosto, 1987; Luosto et al., 1989, 1990, 1994; Yliniemi et al., 1996; Luosto, 1997; Fennia Working Group, 1998; Heikkinen and Luosto, 2000). P- and S-wave velocities were extracted from the original ray-tracing models. Fig. 2a shows an example of the velocity models and Fig. 2b the original seismic data on which the model is based. The model and data are from the profile SVEKA'81.

Laboratory measurements of velocities measured as functions of temperature and pressure are available in the literature for a wide range of different rock types.

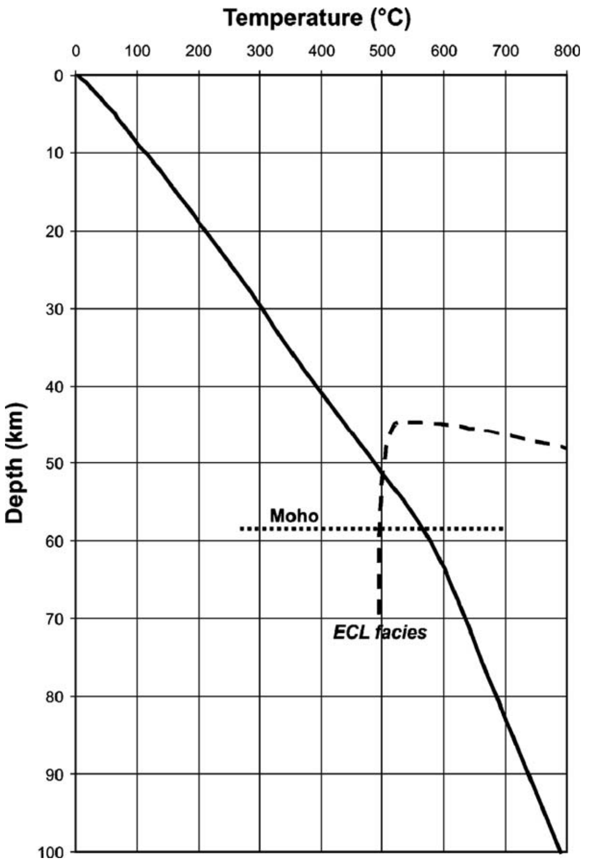

Fig. 3. Geotherm for the central part of the Fennoscandian Shield derived from a lithospheric heat transfer model calibrated with PT data on kimberlite-hosted mantle xenoliths (Kukkonen et al., 2003). The dotted line indicates the Moho depth on the BALTIC transect (Luosto et al., 1990) in the area of kimberlite occurrences in eastern Finland and the broken line indicates the stability field of eclogite facies rocks (adapted from Brown et al., 2003).

Here we applied P-wave velocity measurements taken from Christensen and Mooney (1995) and the V_P/V_S ratios from Christensen (1996). The laboratory velocities were corrected for the Finnish conditions using a xenolith-calibrated geotherm (Kukkonen et al., 2003) representative for the central Fennoscandian Shield (Fig. 3). This geotherm gives slightly higher temperature values than the 'low heat flow geotherm' of Christensen and Mooney (1995). Velocities corrected according to the Finnish geotherm were calculated at intervals of 5 km and they were interpolated from Christensen and Mooney's (1995) velocity results for geotherms representing the 'low' and 'average' heat flow.

3. Results

3.1. Velocity trends

P-wave velocities derived from the ray-tracing models of each wide-angle transect are compared with a selection of rock type velocities in Fig. 4. When plotted as functions of depth, the velocities form distinct layers with step-wise increases at layer boundaries (Figs. 2a and 4a–e) as is expected for any ray-traced crustal section. Further, within the major crustal layers, conspicuous trends of increasing velocities are observed. Parts of the layer boundaries can be mapped with wide-angle reflections (see Fig. 2a).

Observation of the refracted waves over a long offset range indicates that, in most cases, a weak positive velocity gradient must exist. However, the velocity gradients within the layers are not precisely constrained by the relatively sparse refraction/wide-angle reflection data (shot point interval typically 60–80 km and station spacing 1–2 km). However, when denser wide-angle data are available, it seems to be possible also to determine velocity structure within the layers more accurately, for example using waveform tomography (Hole et al., 2005; Pratt, 1999), providing in the future better chances for lithological interpretation of seismic results.

When the wide-angle model velocities are compared with laboratory measurements of different rock types, a distinct contrast between the two data sets is observed (Fig. 4). The velocities from wide-angle models show velocities increasing downward, whereas the velocities of single rock types increase in the uppermost 15 km, but become constant or even decrease at deeper levels down to the base of the crust. The increasing trend in the uppermost 15 km is commonly attributed to closure of cracks under pressure (e.g., Christensen, 1996). The velocity behaviour at depths deeper than 15 km is controlled by the pressure and temperature dependencies of velocities. The lack of increasing velocities at depths below the upper crust is a common result for almost all rock types included in the present study. The only exceptions are andesite, basalts, mica quartz schist, slate, diorite, metagraywacke and serpentinite, which show a mild increase of V_P with depth, but the increase is much smaller than the velocity trends in the ray-tracing models. The results indicate that no single rock type is able to provide the downward increasing trends within different crustal layers. Assuming that the velocities from wide-angle models are representative of the real in situ velocities, there must be gradual

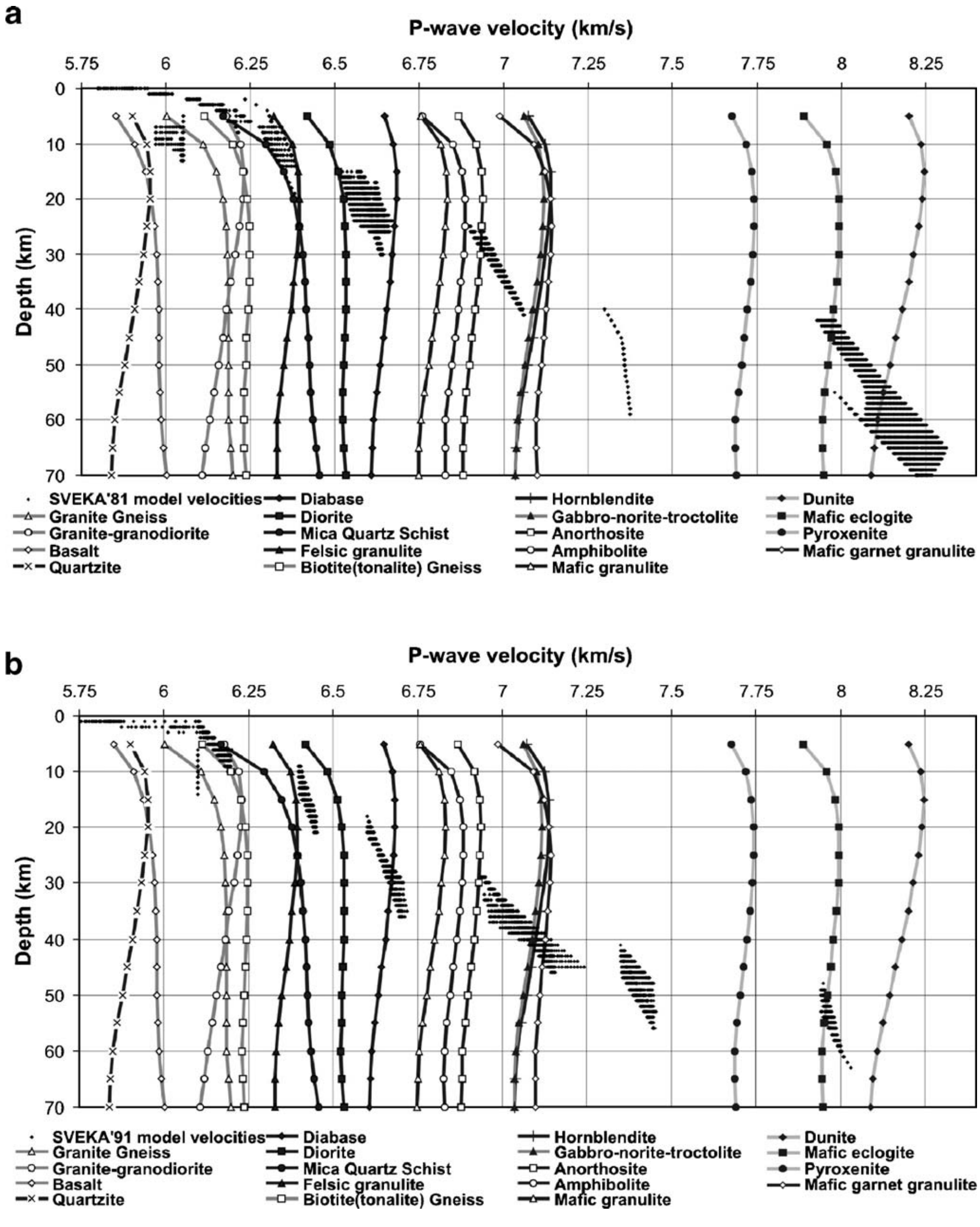

Fig. 4. P-wave velocities of some rock types (lines with symbols) at PT conditions of the Finnish crust together with (a) wide-angle model velocities (dots) from SVEKA'81, (b) SVEKA'91, (c) BALTIC, (d) FENNIA and (e) POLAR. Wide-angle model velocities were picked at 1-km intervals in the vertical and 4-km intervals in the horizontal direction. Vertical overlapping of velocities at boundaries of major velocity layers is due to lateral variations of layer thicknesses. In SVEKA'81, we have included also velocity data from the ray-tracing model of profile extension to NE (Yliniemi et al., 1996; Heikkinen and Luosto, 2000).

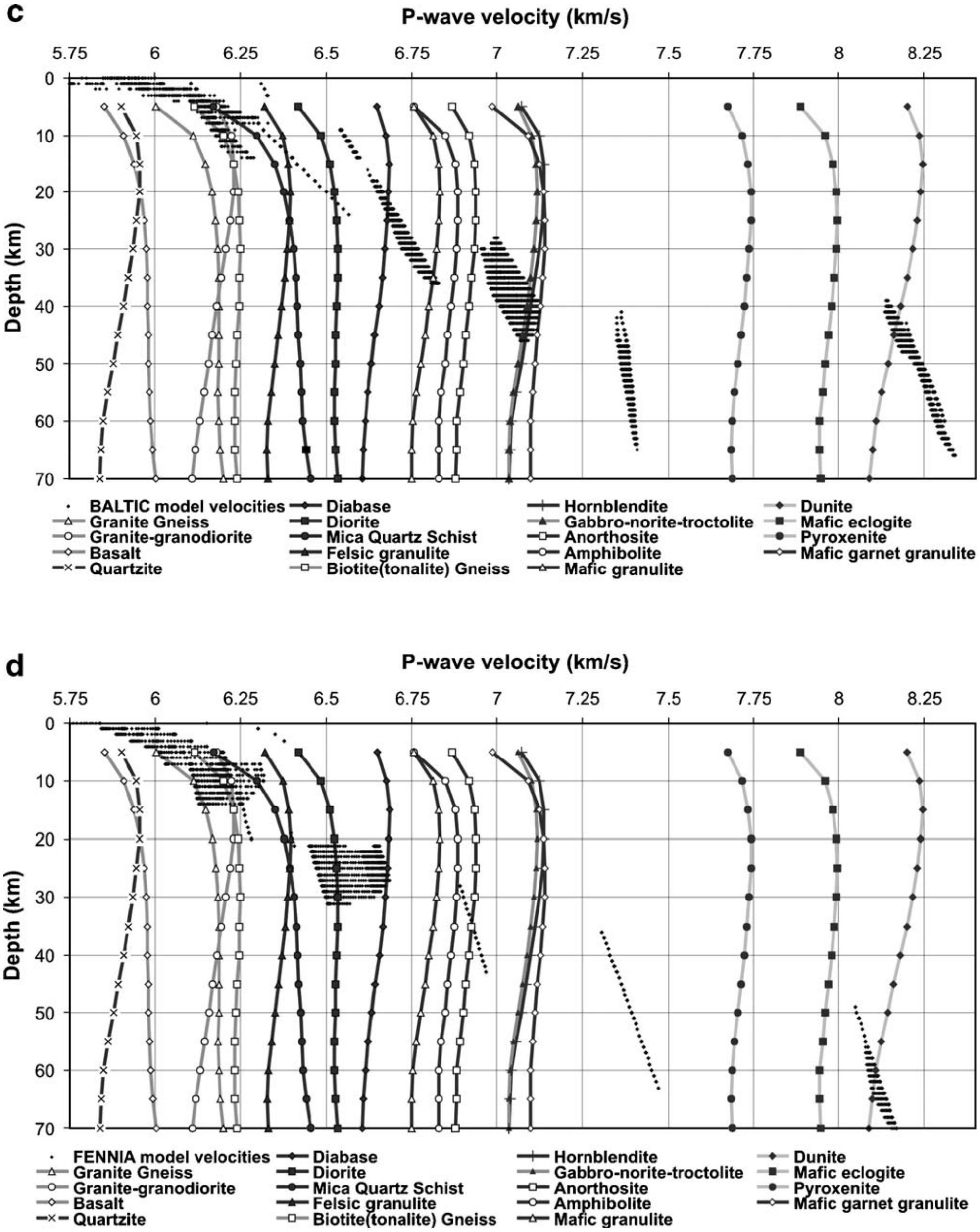

Fig. 4 (*continued*).

vertical changes in rock composition. This increase with depth indicates that the composition of the crust becomes gradually more mafic within the major crustal layers and that the compositional changes in the crust are not limited to major layer boundaries only.

3.2. V_P/V_S ratios

Seismic wide-angle models (Grad and Luosto, 1987; Luosto et al., 1990, 1994; Luosto, 1997; Korsman et al., 1999) show that V_P/V_S ratios range from 1.68 to 1.73 in the upper crust, from 1.73 to 1.76 in the middle crust and from 1.77 to 1.78 in the lower crust. In the upper mantle, V_P/V_S ratio is typically 1.78. The V_P/V_S values from ray-tracing models are supported by similar values obtained in a recent tomographic study of the area (Tiira et al., 2004). The general increasing trend of V_P/V_S ratio in the crust is an indication of the composition becoming more mafic with depth (Christensen, 1996).

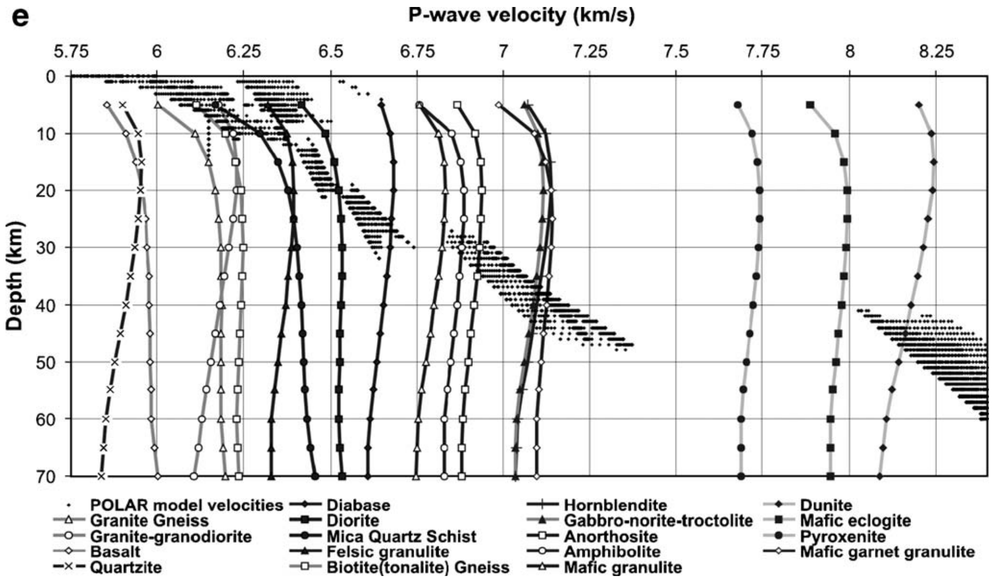

Fig. 4 (*continued*).

3.3. Lower crustal xenoliths

Thirty-four lower crustal xenoliths were recovered from eastern Finland kimberlites (Hölttä et al., 2000; Peltonen et al., in press). Most of them are mafic garnet granulites, but there are also few tonalitic, pyroxenitic and horblenditic rocks (Table 1). The mafic garnet granulites for which thermobarometry was possible represent crystallization temperatures of ca. 800–900 °C and pressures of 0.75–1.25 GPa. Thus, they represent the depth range of about 25–41 km. It should be taken into account that the PT conditions of the pyroxenites, hornblendites and tonalitic granulites, also present in the lower crustal xenolith suite, remain unclear due to lack of suitable mineral pairs for PT determination. Peltonen et al. (in press), nevertheless, consider these rocks to originate from the lower crust because of mineralogical and textural evidence.

We have calculated the seismic velocities and V_P/V_S ratios of these xenoliths from their modal rock compositions (Hölttä et al., 2000; Peltonen et al., in press) using the software of Hacker and Abers (2004) (Table 1). The original samples do not allow laboratory measurements due to their small size and condition. Calculated P-wave velocities (for 970 MPa and 347 °C, corresponding to the depth of 35 km along the geotherm in Fig. 3) vary from 6.3 km/s to 7.5 km/s, with an average of 7.1 km/s. S-wave velocities vary from 3.4 km/s to 4.2 km/s, with an average of 4.0 km/s, respectively. Biotite and quartz-bearing xenoliths have lower velocity values than other xenoliths. V_P/V_S ratios vary from 1.70 to 1.86 (average 1.79). Biotite-bearing xenoliths have higher V_P/V_S ratios, whereas quartz-bearing rocks have lower V_P/V_S ratios than the other (mostly mafic) xenoliths. For the mafic garnet granulites, the results of velocity calculations are in a good agreement with mafic garnet granulite data of Christensen and Mooney (1995) and Christensen (1996).

3.4. Lithological models

Even though single rock types cannot simulate the wide-angle model velocities, it can be done with a mixture of rock types. There are a large number of rock type mixtures giving the correct velocities. Therefore, the inverse solution of rock types and their proportions from velocities is a non-unique problem if only seismic velocity data is available. This is further complicated by the fact that lateral resolution is relatively poor in wide-angle soundings. The velocity models provide only averaged velocity information over wide areas and the velocity layers probably inherently represent combinations of rock types. We limit the present study in forward modelling guided with available geological knowledge.

To constrain the possible lithological types in different crustal layers, we have calculated P-wave velocities, V_P/V_S ratios and densities of different plausible mixtures of rock types and fitted them with the wide-angle velocity models. The averages were calculated as arithmetic means weighted with the rock

Table 1
Modal composition and calculated V_P velocities and V_P/V_S ratios of lower crustal xenoliths recovered from eastern Finland kimberlites

Sample [a]	Rock type [a]	Modes [b]	V_P (km/s) [c]	V_P/V_S ratio [c]
7-HH	Mafic garnet granulite	$Gt_{15}Cpx_{38}Af_4$ $Pl_{42}Op_3$	7.244	1.792
30-A-HH	Mafic granulite	$Cpx_{68}Bt_{27}Chl_4$	6.924	1.809
30B/1-HH	Mafic garnet granulite	$Gt_3Cpx_{29}Pl_{29}Bt_{35}Chl_4$	6.411	1.838
30B/2-HH	Granulite	$Opx_1Pl_{60}Af_{25}Chl_{13}Op_1$	6.702	1.803
31-HH	Mafic garnet granulite	$Gt_1Cpx_7Af_{64}Pl_{12}Chl_{15}$	7.073	1.774
L-31	Mafic garnet granulite	$Gt_2Cpx_9Af_{62}Pl_{25}Chl_2$	7.061	1.785
L-32	Mafic granulite	$Cpx_6Af_{69}Pl_{23}$	7.013	1.784
L-34	Mafic garnet granulite	$Gt_{13}Cpx_1Af_{62}Pl_{15}Chl_6$	7.187	1.778
L-72	Mafic garnet granulite	$Gt_{17}Cpx_{39}Af_{15}Pl_{27}Chl_2$	7.395	1.785
L-73	Mafic garnet granulite	$Gt_9Cpx_{16}Af_{52}Pl_{19}Chl_3$	7.284	1.787
L-86	Mafic garnet granulite	$Gt_{14}Cpx_{29}Af_{25}Pl_{30}$	7.277	1.787
L-87	Mafic garnet granulite	$Gt_{18}Cpx_{32}Af_9Pl_{33}Op_7$	7.343	1.793
L-88	Mafic garnet granulite	$Gt_{13}Cpx_7Af_{19}Pl_{54}Chl_4Op_2$	6.950	1.802
L-90	Mafic garnet granulite	$Gt_{17}Pl_{37}Bt_{44}$	6.274	1.857
L-91	Mafic garnet granulite	$Gt_{19}Cpx_{27}Af_{32}Pl_{19}Op_3$	7.412	1.783
L-93	Mafic garnet granulite	$Gt_{28}Cpx_{23}Af_{25}Pl_{14}Chl_1Op_6Qz_1$	7.537	1.779
L-94	Mafic garnet granulite	Gt_{27} Cpx_{29} $Af_{11}Pl_{26}Op_5Qz_2$	7.484	1.784
L-102	Garnet granulite	$Gt_2Af_{20}Pl_{55}Bt_1Chl_7Qz_6$	6.628	1.785
L-104	Mafic granulite	$Cpx_{16}Opx_{19}Pl_{48}Bt_{14}Qz_2$	6.574	1.804
L81	Mafic garnet granulite	$Gt_{17}Cpx_{47}Af_1Pl_{27}Op_3Qz_3$	7.326	1.765
X001	Mafic garnet granulite	$Gt_{21}Cpx_{32}Af_{10}Pl_{32}Op_6$	7.320	1.782
L23	Mafic garnet granulite	$Gt_{14}Cpx_{30}Af_{10}Pl_{39}Op_6Qz_1$	7.172	1.787
L83	Mafic garnet granulite	$Gt_{22}Cpx_{24}Af_{31}Pl_{20}Op_4$	7.386	1.777
R-38-193	Mafic garnet granulite	$Gt_{15}Cpx_{27}Af_{34}Pl_{21}Op_3$	7.300	1.776
X002	Mafic garnet granulite	$Gt_{26}Cpx_{21}Af_{37}Pl_9Op_7$	7.527	1.775
L84	Mafic garnet granulite	$Gt_{20}Cpx_{11}Af_{47}Pl_{19}Op_3$	7.311	1.780
L85	Mafic garnet granulite	$Gt_{19}Cpx_{26}Af_{47}Pl_5Op_4$	7.473	1.769
X006	Mafic garnet granulite	$Gt_{20}Cpx_4Af_{60}Pl_{17}$	7.289	1.779
Ju11/15.95	Mafic garnet granulite	$Gt_{20}Cpx_{15}Pl_{65}$	6.997	1.803
X208	Granulite (monzodiorite)	$Opx_4Af_2Pl_{63}Bt_6Qz_4Kfp_{19}Op_2$	6.371	1.824
L96	Granulite (tonalite)	$Opx_4Af_{12}Pl_{50}Bt_1Qz_{32}$	6.392	1.704
L89	Pyroxene-hornblende gabbro	$Cpx_7Af_{77}Pl_{14}Op_1$	7.075	1.777
X029	Gabbro	$Cpx_{25}Af_9Pl_{39}Bt_9Op_7Qz_{11}$	6.630	1.767
L82	Hornblende gabbro	$Af_{76}Pl_{22}Op_3$	6.993	1.785

[a] Sample identification, rock type and modal composition were adopted from Hölttä et al. (2000) and Peltonen et al. (in press).
[b] Gt = garnet, Cpx = clinopyroxene, Opx = orthopyroxene, Af = amphibole (hornblende), Pl = plagioclase, Op = opaques, Chl = chlorite, Qz = quartz, Bt = biotite, Kfp = potassium feldspar.
[c] V_P and V_P/V_S ratios were calculated from modal compositions (Hölttä et al., 2000; Peltonen et al., in press) using Hacker's and Abers' (2004) software. In velocity calculations, the accessory minerals (total proportion mostly <3%) were ignored. Velocities were calculated for pressure of 970 MPa and temperature of 347 °C, which correspond to the conditions at the depth of 35 km on the geotherm of Fig. 3.

type proportions. The results from SVEKA'81 for P-wave velocities are shown in Fig. 5a–c, for V_P/V_S in Fig. 6 and for density in Fig. 7. It should be noted here that the available laboratory measurements limit the possible rock type assortment. Due to the non-unique character of the problem, choices must be done in selecting the rock types to be included in the models. For instance, we have done this for upper crustal compositions using information available on geological maps. However, deeper layers of the crust can be expected to be more mafic to show higher metamorphic grade and possible restitic character. To compare our results with previously published global petrological interpretation on the composition of the continental crust by Christensen and Mooney (1995), we have taken their model of the average crustal composition (CM95) as a starting model in the present modelling. An example of these results is shown for the SVEKA'81 transect. It is obvious that the crustal composition on SVEKA'81 does not agree with the global average (Fig. 5a). The SVEKA'81 ray-tracing velocities are about 0.2 km/s higher than the average global lithological model implies.

A modified version of the Christensen and Mooney (1995) model (FINMIX-1) is shown in Fig. 5b. We have not changed the rock type selection from the original CM95 model; the only essential change is the increase of amphibolite proportion in the upper and middle crust. This already suggests that the crust is more mafic in the central Fennoscandian Shield than the global average. Increasing the amphibolite component in the model yields a good fit of P-velocities at depths between 5 and 30 km. The Moho in central Finland is however much deeper (52 km on average) than in the CM95 global average model (40 km). Thus, the CM95 model is not sufficient for modelling the lowermost crust in central Finland. We also need more rock type variation in the upper crust as suggested by the geological maps and the strong seismic reflectivity recorded in the upper crust. The V_P/V_S ratio of the CM95 model is also too high in the lower crust (25–40 km). Therefore, we propose and present here an alternative model (FINMIX-2), which takes into account these issues (Fig. 5c). The upper crust of FINMIX-2 is mostly composed of granite–granodiorite and granitic gneiss, with minor additions of amphibolite, diabase and quartzite. In the middle crust, granitic and tonalitic gneiss and amphibolite dominate.

a

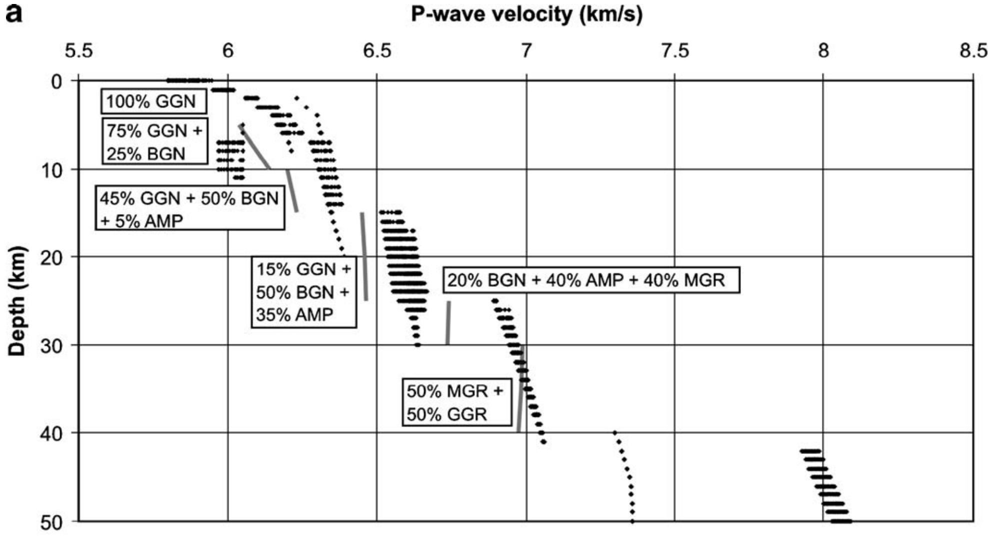

b

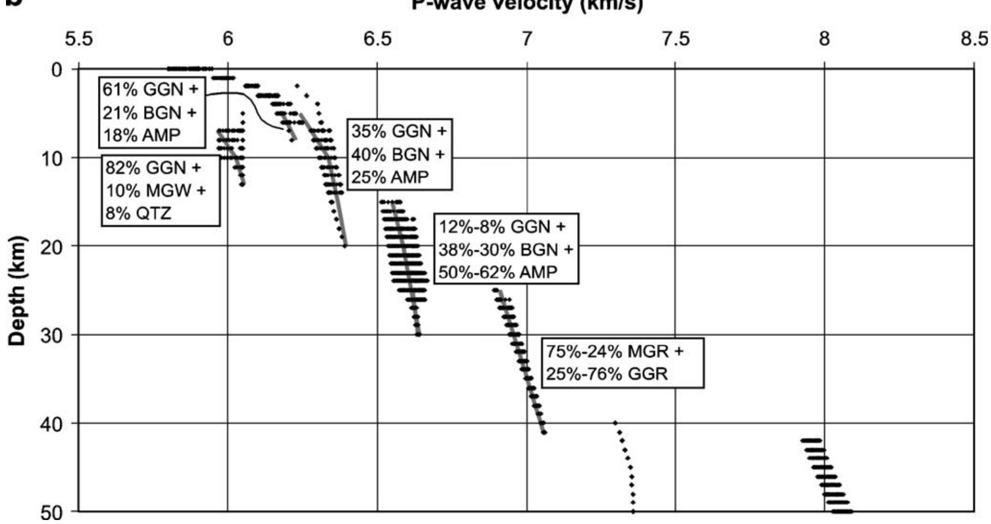

Fig. 5. Modelling of the lithological composition of the crust on the SVEKA'81 transect. P-velocities of the rock type mixtures shown (gray lines) were calculated as arithmetic means of single rock type velocities, corrected according to the PT conditions of the geotherm in Fig. 3 and weighted with rock type proportions applied. The percentage ranges indicate relative proportions of rock types at the upper and lower ends of the corresponding depth intervals. Comparison of the SVEKA'81 velocities with the CM95 model is shown in (a), with FINMIX-1 in (b) and with FINMIX-2 in (c). GGN = granitic gneiss, GRA = granite–granodiorite, BGN = biotite (tonalite) gneiss, QTZ = quartzite, DIA = diabase, AMP = amphibolite, MGW = metagraywacke, MGR = mafic granulite, PYX = pyroxenite, HBL = hornblendite, GGR = mafic garnet granulite and ECL = eclogite.

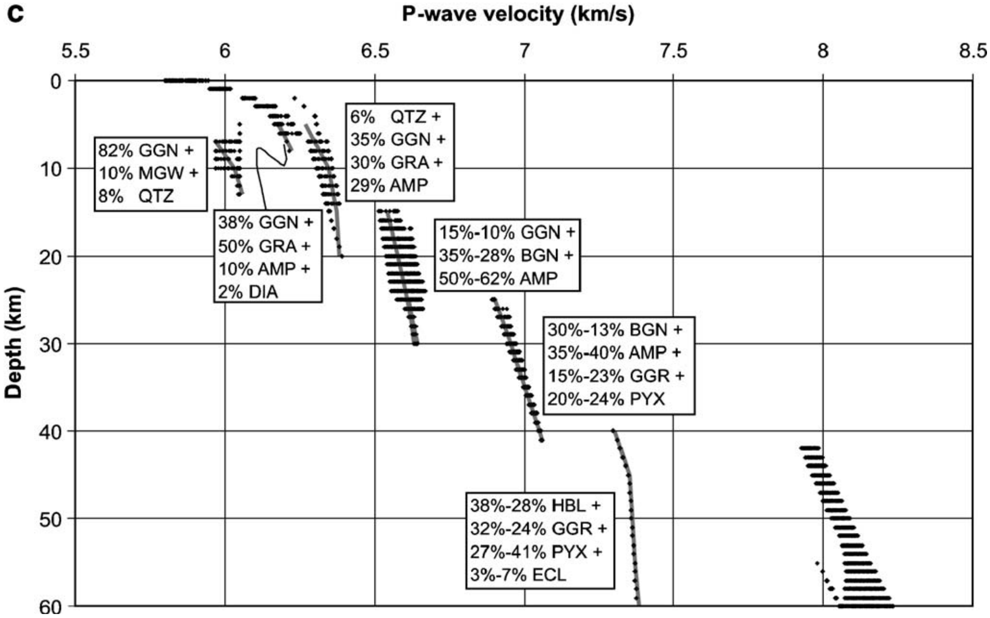

Fig. 5 (*continued*).

Assuming that the upper crustal low-velocity layer is due to variation in composition, it can be interpreted as a mixture of granitic gneiss, metagraywacke and quartzite. However, we should be careful in interpreting the low-velocity layer, which could also be attributed to structural effects.

At deeper levels, in the upper part of the lower crust (25–41 km), a mixture of amphibolite, tonalitic gneiss, mafic garnet granulite and pyroxenite is dominating, whereas the lowermost high-velocity crust (40–59 km) consists of hornblendite, mafic garnet granulite, pyroxenite and mafic eclogite (Fig. 5c).

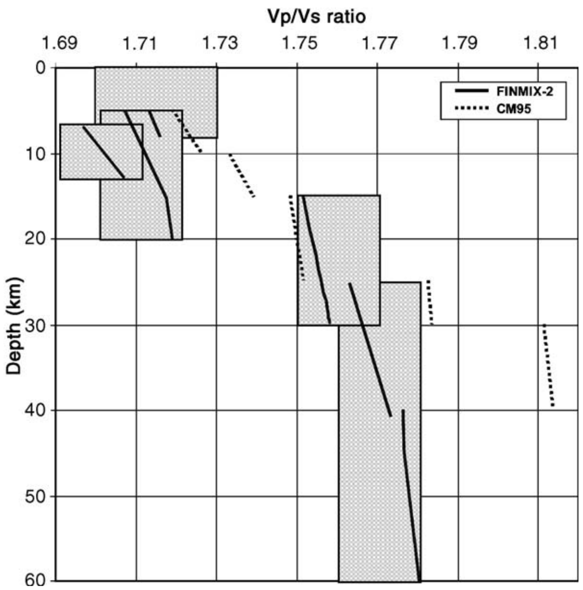

Fig. 6. V_P/V_S ratios on the transect SVEKA'81 calculated using the rock type proportions applied in Fig. 5c (FINMIX-2, solid lines). The grey areas show V_P/V_S ratios with error bounds estimated from the wide-angle model of SVEKA'81 (Grad and Luosto, 1987; Korsman et al., 1999). V_P/V_S ratios of CM95 model (Fig. 5a) are shown for comparison.

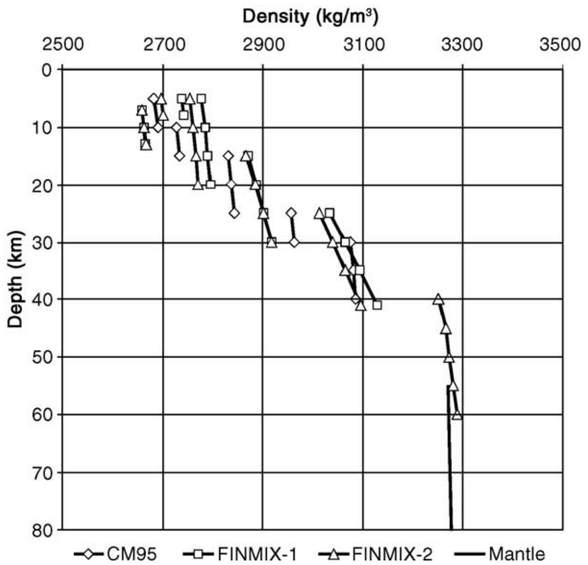

Fig. 7. Vertical density profiles of the crust and upper mantle calculated for the rock type mixtures of the compositional models CM95, FINMIX-1 and FINMIX-2 (Fig. 5a–c).

In addition to SVEKA'81, we have compared the CM95 model with the transects SVEKA'91, FENNIA and BALTIC. Results from these transects suggest that the rock type selection chosen by Christensen and Mooney (1995) generally yields velocities which are too low. In order to increase the velocity levels, we would have to increase the proportion of intermediate and mafic rock types, particularly amphibolite in the middle crust. Only the transect FENNIA in southern Finland would indicate middle crustal compositions more felsic than the CM95 model. These comparisons with CM95 model are, however, complicated by the smoothed character of the average global velocity–depth curve (see Fig. 18 in Christensen and Mooney, 1995), which completely lacks step-like velocity changes. Further, the crustal thickness is only 40 km in the CM95 model, whereas in southern and central Finland the Moho is deeper than 50 km. Therefore, quantitative fitting of the rock type selection of the CM95 model may not provide essentially new information.

3.5. Reflection coefficients

The presence of seismic reflectors at different crustal levels can be used as an indicator of rock type variations, although we must remember that a range of properties including velocity anisotropy, fractures, faults and fluids also produce reflections. By estimating the maximum acoustic reflection coefficients between different rock types included in the velocity models, we can roughly estimate the credibility of the models where crustal scale reflection data is available. We could expect that the major rock types present in the crust should also provide sufficient reflection contrasts in addition to the correct average velocities. In Finland, the new reflection sections of the FIRE transects (Kukkonen et al., 2004) provides a good data set for general comparisons. The FIRE results suggest strong reflectivity throughout the whole crust, with the strongest reflectors generally in the upper and middle crust, whereas the lower crust, particularly in the area of the thick crust in central Finland, shows more diffuse reflectivity (Fig. 9a,b). Moho is not reflective in areas of thick high-velocity lower crust and Moho is indicated only by downward ending of the lower crustal diffuse reflectivity. At Moho depths, the frequency band of FIRE data is limited to frequencies smaller than about 30–40 Hz. Theoretically, the minimum length of detectable reflectors (the Fresnel radius) is about 2 km, when the target is at 40–50 km depth and a signal frequency of 40 Hz is applied in a near-incident reflection survey. Respectively, the theoretical vertical resolution of the same seismic signal can be estimated with the Rayleigh criterion and is of the order of 50 m. In the FIRE-1 section, the lowermost crust is characterized by abundant reflectors ranging from a few hundred metres to 2–3 km in length and from

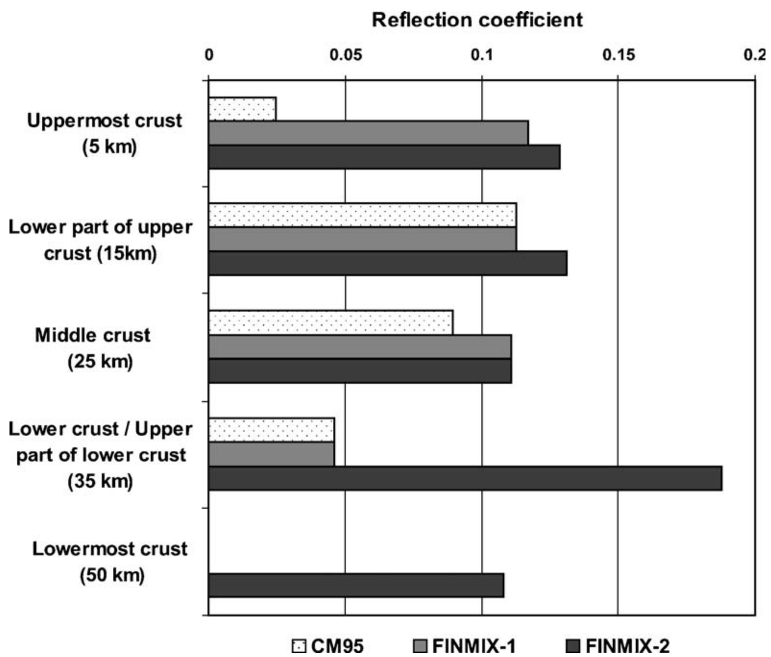

Fig. 8. Maximum reflection coefficients calculated layer-wise from acoustic contrasts between the rock types applied in the different compositional models (CM95, FINMIX-1 and FINMIX-2; Fig. 5). Representative depths of layers are indicated.

about 150 to 300 m in thickness. It seems that the FIRE reflection data from the lower crust partly indicates true reflectors, but due to short horizontal correlation distances the section contains also back-scattered energy from three-dimensional bodies smaller than the resolution of the method would allow.

The reflection coefficients calculated within the major crustal layers for maximum contrasts between the rock types applied in the different compositional models (CM95, FINMIX-1 and FINMIX-2) are shown in Fig. 8. The CM95 model shows strong reflection coefficients between 10 and 30 km (0.08–0.12), but weak coefficients in the uppermost and lowermost crust (<0.05). On the other hand, the FINMIX-1 model suggests strong reflectivity from the upper crust to 30 km (0.11–0.12), but only weak reflectivity at 30–40 km (0.05). The FINMIX-2 model shows strong reflectivity (0.11–0.18) at all depth levels. Further, reflection coefficients between the major velocity layers are smaller than 0.05 (velocities and densities in Figs. 5 and 7). It implies that the crustal reflectivity is best observed within the major velocity layers, but the layer boundaries would not be easily detected in near-incident reflection surveys.

4. Comparison of wide-angle velocity models with reflection sections

Wide-angle and reflection seismic data often show dramatically different structures in crystalline rock areas. Near-incident reflection sections may show dipping and inclined structures, which cannot be correlated with the velocity models derived from wide-angle recordings. Partly, it can be attributed to the inherent differences between the methods and different aims in processing the data as well as to different spatial resolutions of the methods. Even so, we should expect correlations between reflection and refraction surveys, although complicated structures of the crystalline crust may mislead the interpreter.

We have compared the FIRE-1 and FIRE-3 reflection sections with the wide-angle velocity model of SVEKA’81 (Fig. 9a,b). FIRE-1 runs roughly parallel to the SVEKA’81 profile (Fig. 1) at a distance of less than 40 km from the wide-angle transect and provides a good case for comparing the two different data sets. Comparison of the SVEKA’81 model projected on the FIRE-1 transect shows that generally there is only a weak correspondence of the reflectors and velocity boundaries (Fig. 9a). The velocity model does not correspond to the inclined reflectors characteristic for the FIRE-1 transect.

We attribute the lack of correlation between FIRE-1 reflectors and SVEKA’81 velocity model to the fact that the reflection structures are actually three-dimensional. The SVEKA’81 transect does not run perpendicularly to the reflection structures in the crustal scale, although it crosses the geological surface boundaries at angles close to perpendicular. In Fig. 9b, we compare the reflection structures revealed by FIRE-1 and FIRE-3, and the velocity model of SVEKA’81 in the crossing area of the transects. The uppermost velocity layer of SVEKA’81 (0–ca. 10 km) is characterized by sharp, well focused, inclined reflectors on the FIRE sections. The low-velocity layer at 7–10 km on SVEKA’81 can be correlated with the base of a strong low-angle reflector dipping about 10°SE on FIRE-3. The projection of the same reflector is horizontal on FIRE-1. The middle crust with two velocity layers (10–19 km and 19–28 km) is not reflective at this part of FIRE-3. At deeper layers, the upper part of the lower crust (28–40 km) is seen as a reflective layer in FIRE-3 and the projection of the reflector on FIRE-1 indicates that the structure is dipping south with an angle of about 15 degrees. In contrast, the lowermost crust (40–58 km) is represented by diffuse reflectivity on both FIRE sections. Moho is not reflective on FIRE-1 or FIRE-3 in Fig. 9b.

According to the FINMIX-2 model (Fig. 5c), the upper crustal reflectivity can be attributed to amphibolite and diabase in a granitic–granodioritic environment. The middle crustal reflectivity would be produced by amphibolite within granitic and tonalitic gneisses. The upper part of the lower crust (25–41 km, Fig. 5c) contains tonalitic gneisses, together with amphibolite, mafic garnet granulite and pyroxenite, which implies strong reflection coefficients between the co-existing rock types in this layer. The diffuse reflectivity in the high-velocity lowermost crust is attributed to hornblendite, pyroxenite, mafic garnet granulite and mafic eclogite. In the lowermost crust (>40 km), tonalitic rocks are not present, which decreases the predicted maximum reflection coefficients, but this is partly compensated by mafic eclogite. We attribute the lack of strong reflectors in the lowermost crust in FIRE sections (Fig. 9b) to the small dimensions of rock type blocks and short correlation distances between them, resulting in a structure below the resolution limit of the technique.

Generally, comparison of velocity models and reflection sections should be done with great care. We should avoid projecting velocity models on reflection sections without any control of possible three-dimensionality of the structures. In the present

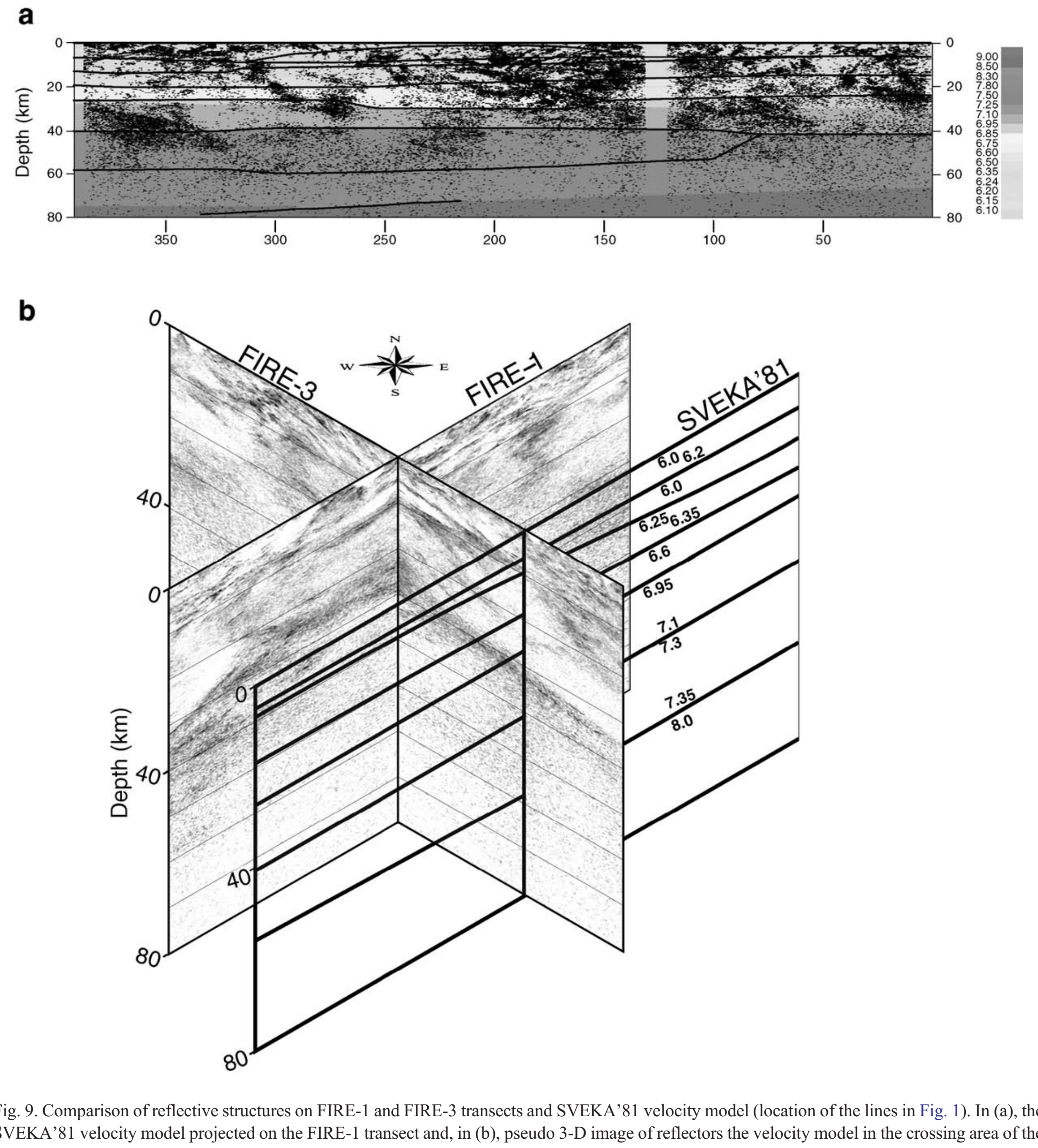

Fig. 9. Comparison of reflective structures on FIRE-1 and FIRE-3 transects and SVEKA'81 velocity model (location of the lines in Fig. 1). In (a), the SVEKA'81 velocity model projected on the FIRE-1 transect and, in (b), pseudo 3-D image of reflectors the velocity model in the crossing area of the transects (vertical/horizontal scale 1:1).

case, the distance of about 30–40 km between the FIRE-1 and SVEKA'81 was already too long for reliable comparison of the different data sets (Fig. 9a). Although typical crooked-line geometry provides a means to recognize 3-D structures, the crossing of FIRE-1 and FIRE-3 transects was vital for understanding the real geometry of crustal structures in central Finland.

5. Discussion

The lithological modelling of crustal velocities is a non-unique problem when only seismic velocity data is available. Nevertheless, such modelling allows constraining the possible compositions of the crust if the major rock types can be selected using additional information including direct geological observations, deep drillings in the upper crust, gravity and magnetic models, or crustal xenoliths brought to surface by volcanic rocks or kimberlites.

Already the seismic data itself can reduce the number of solutions. Where V_P/V_S ratios are available, the compositional ambiguity can be reduced. In the present study, the V_P/V_S data from the wide-angle models provided useful constraints in modelling. Particularly, the range of compositions of the lower crust in central Finland could be narrowed down with V_P/V_S data. For instance, the compositional model FINMIX-2 suggests that the lowermost crust is a mixture of hornblendite, mafic garnet granulite, eclogite and pyroxenite. The result is in agreement with deep crustal kimberlite-hosted xenolith data in eastern Finland (Hölttä et al., 2000; Peltonen et al., in press).

The correction of seismic velocities measured in the laboratory was based on the xenolith-corrected geotherm presented by Kukkonen et al. (2003). The geotherm is strictly valid only in eastern Finland near the Archaean–Proterozoic boundary. However, it probably represents the central Fennoscandian Shield very well within a maximum error of ±50 K (see also Kukkonen et al., 1999 for a discussion on reliabilities of geothermal models). For instance, in the lowermost crust, such a temperature difference would indicate an uncertainty smaller than about 0.03 km/s (V_P) for a mafic garnet granulite and 0.02 km/s for a tonalite, respectively. We may conclude that the uncertainties in temperature estimation do not play an essential role in a stabilized cratonic area.

A major observation in the present study is the gradual P-velocity increase with depth within the major crustal layers. We attribute this to the rock composition becoming gradually more mafic within the layers. It could represent compositional trends originally produced by partial melting and subsequent removal of felsic melts to higher levels in the lithosphere. The deeper sections would have experienced higher degrees of melting, which would make them more mafic with faster velocities today.

The observed velocity trends within crustal layers may also be due to natural variations of velocities with increasing pressure and temperature. As reported in earlier studies, single rock types are not able to explain the downward increasing velocities in the crustal scale (Rudnick and Fountain, 1995; Christensen and Mooney, 1995). In single layers, however, the existence of velocity trends in modelled rock type velocities will depend on the applied PT corrections, because seismic velocities decrease with increasing temperature, but increase with increasing pressure.

The total effect is quite sensitive to the applied derivatives. Laboratory measurements of seismic velocities are usually carried out from room temperature to about 700–800 °C, to represent conditions in the crust and upper mantle in cratonic areas; however, the pressure ranges often only up to about 600 MPa, which corresponds to a depth of about 22 km. Pressure dependencies deeper than this are usually extrapolated from the measured data. Rudnick and Fountain (1995) used data measured to 600 MPa and compared the velocity trends calculated for mafic and felsic single rock types under either a low (40 mW m^{-2}) or a high geotherm (90 mW m^{-2}). Their result indicates that there should be a slight increase of velocity with depth in the low geotherm case for a single rock type. On the other hand, the results by Christensen and Mooney (1995) and those calculated in the present study for a similar geotherm suggest that velocities would increase at shallow (<15 km) depths, but keep practically constant or even slightly decrease at deeper levels to the base of crust. We attribute this to different pressure ranges applied in the original laboratory measurements in Rudnick and Fountain's (1995) data set than in the Christensen and Mooney's (1995). Christensen and Mooney derived their pressure derivatives from measurements up to 1 GPa, which resulted in slightly smaller pressure derivative values.

According to the mantle-xenolith calibrated geotherm (Fig. 3), the deepest part of the crust (ca. deeper than 55 km) is in conditions of eclogite facies. However, during active stages of crustal development, when the geotherm was steeper during the Svecofennian orogeny at about 1.9–1.8 Ga ago, the thickened crust could well have reached eclogite facies conditions at depths exceeding 45 km. This would have allowed transformation of rocks with basaltic–gabbroic composition into eclogite. During orogenic collapse, thick layers of high-density eclogite would most probably have delaminated into the mantle. Part of the eclogitized rocks may have remained in the crust, but with geotherm cooling after the orogenic peak, a retrogressive transformation back to granulites would have taken place. Such a reaction is not necessarily complete and small amounts of eclogite could still exist in the lower crust.

So far, crustal eclogites have not been recovered in the kimberlite-hosted xenoliths in Finland. It could be attributed to the very small number of lower crustal xenoliths recovered altogether suggesting that sampling of the lower crust by the available xenoliths may not be representative. Alternatively, the lack of eclogites could be due to rock-type dependent differences in the mining of sidewall rocks during kimberlite uplift. However, mafic eclogites are a relevant component required in the FINMIX-2 model to explain the high P-velocity and low V_P/V_S ratio of the lowermost crust.

An important implication is obtained by calculating the density profile of the crust of the FINMIX-2 model (Fig. 7). The lowermost crust attains a density value of about 3290 kg/m^3 at the depth of ca. 50 km. The calculated upper mantle density (for 1530 MPa and 540 °C, corresponding to the depth of 55 km along the geotherm in Fig. 3), calculated with the average mantle xenolith modal composition (Kukkonen et al., 2003), is 3270 kg/m^3. Although there are uncertainties in the velocity calculations, the results suggest that the lowermost crust has practically no density contrast with the mantle. In terms of seismic reflectivity, this would indicate that the reflection coefficient between the crust and mantle would be quite low because all reflectivity would be produced by the velocity contrast, which is weak. For instance, on SVEKA'81 in the area of thick high-velocity lower crust, the lowermost crust has V_P values varying from 7.35 to 7.45 km/s and the upper mantle beneath Moho 8.08 to 8.30 km/s, respectively. The corresponding reflection coefficients (assuming no density contrast) are of the order of 0.045–0.055. This is in agreement with the fact that Moho boundary is not reflective in central Finland in the FIRE reflection sections (Kukkonen et al., 2004; Fig. 9b).

Further, we propose that the crustal thickness in the central Fennoscandian Shield has been controlled by the densities of the lower crustal and upper mantle rocks. In a simple model, thick layers of high-density rocks (such as eclogite) formed during collision and thickening can be expected to sink into the mantle, whereas anything lighter would float on or above the Moho.

The present models allow calculation of an estimate of the average chemical composition of the crust if the chemical composition of the rock types were available. Unfortunately, Christensen and Mooney (1995) did not report the rock type compositions of the samples in their laboratory velocity compilation. An alternative approach would be to start from mineral compositions of different typical rock types and their modal compositions, and to calculate velocities of rock type mixtures, as well as the chemical compositions (e.g., Hynes and Snyder, 1995). However, we have preferred in this study to apply experimental data on rock velocities in modelling of crustal velocities.

We can conclude that the crust in the central part of the Fennoscandian Shield is more mafic than the average continental crust as seen in comparison of the CM95 and FINMIX-1 and -2 models. This conclusion is also supported by the fact that the crust in the central Fennoscandian Shield is anomalously thick, but there is no topography related to the thick crust. The area is apparently in an isostatic equilibrium (ignoring the postglacial uplift effects). The area of thick crust in the central part of the shield would be expected to exhibit a distinct Bouguer minimum, but actually, there is a weak Bouguer maximum (Elo, 1997). Therefore, the lower crust, beneath a depth of about 40 km, very probably represents dense, mafic rock types, which we have interpreted here as hornblendite, mafic garnet granulite, pyroxenite and mafic eclogite. Same rock types have been recovered from a suite of kimberlite-hosted lower crustal xenoliths in eastern Finland, but so far the sparse xenolith data has indicated nothing about possible crustal eclogites (Hölttä et al., 2000; Peltonen et al., in press).

6. Conclusions

Seismic velocity data in the central Fennoscandian Shield indicate that the crust is composed of distinct velocity layers as would be expected in any case history of continental crust. P-wave velocity, however, gradually increases within the major velocity layers. Such trends cannot be modelled using velocities from single rock types corrected for Fennoscandian Shield PT conditions. We therefore interpret the trends indicating gradual changes in composition with depth, i.e., the rocks become more mafic with increasing depth. The calculated vertical velocity profiles for a range of possible crustal lithological compositions suggest that the Finnish crustal velocities do not agree with the average global continental model of Christensen and Mooney (1995), but require a more mafic composition.

On the SVEKA'81 transect the calculated lithological model (FINMIX-2) suggests that the crustal velocity profiles can be simulated using rock type mixtures in which the upper crust consists of felsic gneisses and granitic–granodioritic rocks with a minor contribution of amphibolite, diabase and quartzite. In the middle crust, the amphibolite proportion increases. The upper part of the lower crust (ca. 25–40 km) is tonalitic gneiss, amphibolite, mafic garnet granulite and pyroxenite, whereas the lowermost part of the lower crust (ca. 40–59 km) is mostly hornblendite, mafic garnet granulite, pyroxenite and mafic eclogite. Data on kimberlite-hosted lower crustal xenoliths recovered from eastern Finland are in agreement with the lithological modellings presented here. The rock types used in compositional modelling have sufficiently high acoustic reflection coefficients to generate the well-developed reflectivity recorded in the crust in the central part of the shield.

Comparison of reflectors from FIRE-1 and FIRE-3 transects and the velocity model from SVEKA'81 wide-angle transect indicated that the reflectors correlate with velocity layering, but the three-dimensional structures of the crust complicate such comparisons.

The density profile calculated from the lithological model of SVEKA'81 wide-angle model velocities suggests that the lower crust attains values, which are very close to upper mantle densities at the Moho level. This implies that crustal thickness in the central Fennoscandian Shield may have been controlled by the densities of the lower crustal and upper mantle rocks.

Acknowledgements

We are grateful to U. Luosto and T. Tiira (Institute of Seismology, University of Helsinki) for discussions on wide-angle velocity models and the possibility to use the original ray-tracing models in this study; to S. Elo (Geological Survey of Finland, Espoo) for discussions on gravity anomalies and density models; and P. Peltonen (Geological Survey of Finland, Espoo) for discussions on xenoliths. The manuscript benefited from reviews by D. Snyder (Natural Resources Canada, Ottawa), G. Musacchio (Queen's University, Kingston, Ontario, Canada) and an anonymous referee. The first author was supported by grants received from the Finnish Academy of Science and Letters, Vilho, Yrjö and Kalle Väisälä Foundation.

References

Brown, D., Carbonell, R., Kukkonen, I., Ayala, C., Golovanova, I., 2003. Composition of the Uralide crust from seismic velocity (V_P, V_S), heat flow, gravity and magnetic data. Earth Planet. Sci. Lett. 210, 333–349.

Christensen, N.I., 1996. Poisson's ratio and crustal seismology. J. Geophys. Res. 101, 3139–3156.

Christensen, N.I., Mooney, W.D., 1995. Seismic velocity structure and composition of the continental crust: a global view. J. Geophys. Res. 100 (B7), 9761–9788.

Elo, S., 1997. Interpretations of the gravity anomaly map of Finland. Geophysica 33, 51–80.

Fennia Working Group, 1998. P- and S-velocity structure of the Baltic Shield beneath the FENNIA profile in southern Finland, Report S-38, University of Helsinki, Institute of the Seismology, Finland. 14 pp.

Grad, M., Luosto, U., 1987. Seismic models of the crust of the Baltic Shield along the SVEKA Profile in Finland. Ann. Geophys. 5B (6), 639–650.

Hacker, B.R., Abers, G.A., 2004. Subduction factory 3. An Excel worksheet and macro for calculating the densities, seismic wave speeds, and H_2O contents of minerals and rocks at pressure and temperature. Geochem. Geophys. Geosyst. G3 5 (1), Q01005, doi:10.1029/2003GC000614.

Heikkinen, P., Luosto, U., 2000. Review of some features of the seismic velocity models in Finland. In: L.J. Pesonen, A. Korja and S.-E. Hjelt, (eds.). Lithosphere 2000—A Symposium on the Structure, Composition and Evolution of the Lithosphere in Finland. Espoo, Finland, Oct. 4–5, 2000. Institute of Seismology, University of Helsinki, Report S-41, 35–41.

Holbrook, W.S., Mooney, W.D., Christensen, N.I., 1992. The seismic velocity structure of the deep continental crust. In: Fountain, D.M., Arculus, R., Kay, R.W. (Eds.), Continental Lower Crust. Elsevier, Amsterdam, pp. 1–43.

Hole, J.A., Zelt, C.A., Pratt, R.G., 2005. Advances in controlled-source seismic imaging. EOS Trans. Am. Geophys. Union 86, 177–181.

Hölttä, P., Huhma, H., Mänttäri, I., Peltonen, P., Juhanoja, J., 2000. Petrology and geochemistry of mafic granulite xenoliths from the Lahtojoki kimberlite pipe, eastern Finland. Lithos 51, 109–133.

Hynes, A., Snyder, D.B., 1995. Deep-crustal mineral assemblages and potential for crustal rocks below the Moho in the Scottish Caledonides. Geophys. J. Int. 123, 323–339.

Kern, H., 1978. The effect of high temperature and high confining pressure on compressional wave velocities in quartz-bearing and quartz-free igneous and metamorphic rocks. Tectonophysics 44, 185–203.

Korja, A., Korja, T., Luosto, U., Heikkinen, P., 1993. Seismic and geoelectric evidence for collisional and extensional events in the Fennoscandian Shield—implications for Precambrian crustal evolution. Tectonophysics 219, 129–152.

Korsman, K., Korja, T., Pajunen, M., Virransalo, P., GGT/SVEKA Working Group, 1999. The GGT/SVEKA transect: structure and evolution of the continental crust in the Palaeoproterozoic Svecofennian orogen in Finland. Int. Geol. Rev. 41, 287–333.

Kukkonen, I.T., Jokinen, J., Seipold, U., 1999. Temperature and pressure dependencies of thermal transport properties of rocks: implications for uncertainties in thermal lithosphere models and new laboratory measurements of high-grade rocks in the central Fennoscandian Shield. Surv. Geophys. 20, 33–59.

Kukkonen, I.T., Kinnunen, K.A., Peltonen, P., 2003. Mantle xenoliths and thick lithosphere in the Fennoscandian Shield. Phys. Chem. Earth 28, 349–360.

Kukkonen, I.T., Heikkinen, P., Ekdahl, E., Hjelt, S.E., Korja, A., Lahtinen, R., Yliniemi, J., Berzin, R., FIRE Working Group, 2004. FIRE transects: new images of the crust in the Fennoscandian Shield. In: D.B. Snyder, R. Clowes (Compilers), The 11th International Symposium on Deep Seismic Profiling of the Continents and Their Margins, Programme and Abstracts, Mont-Tremblant, Quebec, Canada, 25 Sept.–1 Oct. 2004. Lithoprobe Report no. 84, 65 (abstract).

Lahtinen, R., Korja, A., Nironen, M., 2005. Paleoproterozoic tectonic evolution. In: Lehtinen, M., Nurmi, P.A., Rämö, O.T. (Eds.), Precambrian Geology of Finland: Key to the Evolution of the Fennoscandian Shield. Elsevier Science B.V., Amsterdam, pp. 481–532.

Luosto, U., 1997. Structure of the Earth's crust in Fennoscandia as relieved from refraction and wide-angle reflection studies. Geophysica 33 (1), 3–16.

Luosto, U., Flueh, E.R., Lund, C.-E., Working Group, 1989. The crustal structure along the POLAR Profile from seismic refraction investigations. Tectonophysics 162, 51–85.

Luosto, U., Tiira, T., Korhonen, H., Azbel, I., Burmin, V., Kosminskaya, I., Ionkis, V., Sharov, N., 1990. Crust and upper mantle structure along the DSS Baltic Profile in SE Finland. Geophys. J. Int. 101, 89–110.

Luosto, U., Grad, M., Guterch, A., Heikkinen, P., Janik, T., Komminaho, K., Lund, C., Thybo, H., Yliniemi, J., 1994. Crustal structure along the SVEKA'91 profile in Finland. In: K. Makropoulos and P. Suhadolc (Editors), European Seismological Commission, XXIV General Assembly, 1994 September 19–24, Athens, Greece, Proceedings and Activity Report 1992–1994, Vol.II, 974–983.

Musacchio, G., Mooney, W.D., Luetgert, J.H., 1997. Composition of the crust in the Grenville and Appalachian provinces of North America inferred from Vp/Vs ratios. J. Geophys. Res. 102, 15225–15241.

Musacchio, G., White, D.J., Asudeh, I., Thomson, C.J., 2004. Lithospheric structure and composition of the Archean western Superior province from seismic refraction/wide-angle reflection and gravity modeling. J. Geophys. Res. 109, B03304.

Peltonen, P., Mänttäri, I., Huhma, H., Whitehouse, M., in press. Multi-stage origin of the lower crust of the Karelian Craton from 3.5 to 1.7 Ga based on isotopic ages of kimberlite-derived mafic granulite xenoliths. Precambrian Res.

Pratt, R.G., 1999. Seismic waveform inversion in the frequency domain: Part 1. Theory and verification in a physical scale model. Geophysics 64, 888–901.

Rudnick, R., Fountain, D., 1995. Nature and composition of the continental crust: a lower crustal perspective. Rev. Geophys. 33 (3), 267–309.

Tiira, T., Hyvönen, T., Rautioaho, E., Korja, A., Heikkinen, P., 2004. Tomographic study of seismic velocity structure of the crust in south Finland. In: Snyder, D. (editor) SEISMIX 2004, 11th International Symposium on Deep Structure of the Continents and their Margins, 26.9.–1.10.2004, Quebec, Canada, 105 (abstract).

Yliniemi, J., Jokinen, J., Luukkonen, E., 1996. Deep structure of the Earth crust along the GGT/SVEKA transect extension to northeast. Geol. Surv. Finl., Rep. Investig. 136, 56.